

NON-EQUILIBRIUM PRODUCTION OF PHOTONS VIA

$$\pi^0 \rightarrow 2\gamma \text{ IN DCC's}$$

D. Boyanovsky^(a), H. J. de Vega^(b), R. Holman^(c), S. Prem Kumar^(c)*(a) Department of Physics and Astronomy, University of Pittsburgh, PA.**15260, U.S.A.**(b) LPTHE, Universite' Pierre et Marie Curie (Paris VI), Tour 16, 1er. etage,**4, Place Jussieu 75252 Paris, Cedex 05, France**(c) Department of Physics, Carnegie Mellon University, Pittsburgh, PA.15213, U.S.A.***Abstract**

We study production of photons via the non-equilibrium relaxation of a Disoriented Chiral Condensate with the chiral order parameter having a large initial amplitude along the π^0 direction. Assuming the validity of the low energy coupling of the neutral pion to photons via the $U_A(1)$ anomalous vertex, we find that for large initial amplitudes along the π^0 direction, photon production is enhanced by parametric amplification. These processes are non-perturbative with a large contribution during the non-equilibrium stages of the evolution and result in a distinct distribution of the produced photons and a polarization asymmetry. For initial amplitudes of the π^0 component of the order parameter between 200-400 MeV, corresponding to energy densities between 1-12 GeV/fm³ we find a peak in the photon distribution at energies

between $\approx 300\text{--}600$ MeV. We also find polarization asymmetries typically between $5\text{--}10\%$. We discuss the potential experimental impact of these results as well as the problems associated with its detection.

11.30.Qc, 11.30.Rd, 11.40.Ha

I. INTRODUCTION

The possibility that a disoriented chiral condensate (DCC) might form during the early stages of a high energy, heavy-ion collision, has attracted considerable attention in recent years [1]. The essential idea is that, near the central rapidity region, large energy densities \sim a few GeV/fm³ are achieved, corresponding to temperatures above 200 MeV, at which the chiral symmetry is restored [2]. As this region cools down via hydrodynamical expansion, it is conceivable that the QCD order parameter might be trapped in a configuration where it points in a direction different from the σ direction which corresponds to the true vacuum. Subsequent relaxation of such a DCC configuration to the true vacuum is expected to be accompanied by a strong coherent burst of pions, which would then provide a definitive experimental signature of the chiral phase transition. The formation and relaxation of these DCC configurations could potentially provide an explanation for the CENTAURO and JACEE events found in cosmic ray emulsion experiments [2].

Recent theoretical investigations [3–6] of effective field theories of QCD, particularly the linear sigma model seem to indicate that there is the possibility that such coherent regions may be formed during the non-equilibrium stages of the chiral phase transition. Results of classical [3], semiclassical [4] and quantum calculations, with [5] and without [6] expansion seem to indicate that there is a range of initial conditions for which the chiral phase transition goes through a non-equilibrium stage during which coherent pion clouds like DCC's may be formed.

The telltale experimental signal for DCC events would be a non-binomial distribution for the ratio of the number of neutral pions to the total number of pions $R = n_{\pi^0}/(n_{\pi^0} + n_{\pi^+\pi^-})$ with a probability distribution $P(R) = 1/(2\sqrt{R})$ [2]. Both MINIMAX at the Fermilab Tevatron and WA98 at CERN are currently looking for strong fluctuations in the ratio of neutral to charged pions, and STAR and PHENIX at RHIC are scheduled to search for such

events.

There are potential ambiguities in obtaining clear signals for the probability distribution $P(R)$. Since the emitted pions are strongly interacting objects they will undergo strong final state interactions, and it could be that a DCC signal may be distorted and become indistinguishable from the background. An important limitation for the determination of $P(R)$ is the accounting of neutral pions which decay to two photons before reaching the detector. The neutral pion distribution is typically reconstructed from the analysis of the emitted photons, a very demanding analysis in typical heavy-ion collisions with large multiplicity events.

It is thus important to identify alternative signatures of the chiral phase transition, and DCC formation and relaxation. Electromagnetic probes such as photons and dileptons are ideal candidates since their interactions are weak, and hence they can carry the information from the early stages of the evolution of the plasma with minimal distortion. It is very likely that to extract exotic signals for the chiral phase transition or DCC events, both hadronic and electromagnetic probes will be needed.

Furthermore, with the possibility of non-equilibrium effects during the formation and expansion of the fireball in heavy ion collisions, the study of unusual non-equilibrium processes may provide a greater understanding of the signatures of the Quark-Gluon and Chiral phase transitions in experiments at RHIC and LHC.

In an earlier work [7], we have recently studied direct photon production enhancement from the non-equilibrium relaxation of DCC's. There, we studied the gauged linear sigma model and concentrated on the *electromagnetic interactions of the hadronic current*. These calculations involved the electromagnetic interactions of the charged pions alone. The conclusion of this study was that the total number of photons produced during the non-equilibrium stages of a “quenched” phase transition (which lasts *only for a few fms./c* until the order parameter reaches its equilibrium value), can become comparable to the number of photons

released via (perturbative) decay of *all* the neutral pions produced in the heavy-ion collision (time scale for decay $\sim 10^7$ fm/c).

In this article we focus our attention on the couplings of the *neutral pion only*, to electromagnetism, through the axial anomaly. We work within the framework of the linear sigma model and introduce the anomalous interaction of the π^0 by means of the effective Wess-Zumino-Witten vertex. As described above, a DCC corresponds to a rotation of the chiral order parameter in a coherent domain. Since electromagnetism remains as an unbroken symmetry, such a rotation must be confined to the $\sigma - \pi^0$ plane. A rotation that takes the order parameter out of the neutral meson plane homogeneously, will result in a global breaking of electromagnetism, which is not acceptable. Localized regions in which the charged pion fields obtain (locally) an expectation value (charged droplets) that average to zero on large volumes cannot be ruled out. However, the study of their dynamics involves a non-perturbative treatment of large amplitude inhomogeneous configurations, a very difficult task and beyond the scope of this article. An initial step towards understanding the non-equilibrium evolution of *small amplitude* inhomogeneous configurations was presented in [8].

Minakata and Muller suggested in a recent work [9] that a rotation in the neutral meson plane could indeed be induced in heavy-ion collisions. These authors argue that the presence of strong electromagnetic fields in these collisions will give a “kick” to the chiral order parameter in the π^0 direction, and that this effect is enhanced by the chiral U(1) anomaly. In this scenario, during the initial stages of the collision the order parameter acquires a component in the direction of the neutral pion. This is consistent with the formation of a “chirally disoriented” domain. During the expansion stage this disoriented region cools down and the order parameter relaxes to the true vacuum configuration, with the field oriented in the “ σ ” direction.

The goal of this article is to show that if one begins with the above-mentioned “disori-

ented” initial conditions with a large amplitude component in the π^0 direction, the DCC relaxation will be accompanied by a coherent burst of photons which is released via a *novel non-perturbative mechanism* of parametric amplification, along with with the enhanced pion emission resulting from the non-equilibrium spinodal instabilities.

The essential idea behind this novel mechanism is that the component of the homogeneous order parameter along the π^0 direction (the Fourier mode of the π^0 field with zero spatial momentum) couples to the electromagnetic field through the chiral anomaly, and effectively acts much as a time dependent “mass” term or “squeezing” term for the photon field that leads to the resonances in the equations of motion.

This non-equilibrium mechanism exhibits the features of unstable bands, and exponential growth of the photon mode functions, that are characteristic of parametric resonance. Furthermore, since the amplification and consequently the enhanced photoproduction will be confined only to certain frequency bands, this phenomenon translates into very peculiar distributions for the produced photons. Furthermore, because of the pseudoscalar nature of the interaction, there is a polarization asymmetry in the produced photons, i.e. photons with different polarizations are produced in different amounts. Both features of this non-perturbative mechanism might be potential signatures of DCC’s or similar non-equilibrium relaxation phenomena during the chiral phase transition. Parametric amplification of *pions* has been conjectured to play a role in the hadronization stages of the QGP [10].

In this article we do not incorporate hydrodynamic expansion and treat the dynamics via the “quench” approximation [3,6] from an initial state in local thermodynamic equilibrium above T_c . We also study the evolution of the system from a non-equilibrium initial state at $T_i = 0$ to explicitly show that the qualitative features are robust and not tied to the “quench” scenario. Numerical results of the semiclassical evolution [4] and quantum evolution [5] with expansion reveal that the qualitative features, such as pionic amplification and the estimate of the dynamical time scales are well described by the “quench” scenario.

Our aim in this article is to understand the qualitative aspects of this new mechanism of photoproduction in the simplest of settings, in light of the possibility that it could be a signature of DCC's in heavy ion collisions. A deeper study of these and other photoproduction mechanisms including boost invariant expansion will be presented elsewhere [15].

This article is organized as follows: in Section II, we introduce the model and review the approximations used and their validity. Section III is devoted to a simple derivation of the equations obeyed by the photon mode functions which in turn indicate the nature of the non-perturbative processes of anomalous photoproduction. In Section IV we review the numerical study of the equations of motion, and obtain the photon spectrum for a number of possible initial conditions, and in Section V we discuss some of the experimental implications of these results and potential difficulties for its detection. In Section VI we present our conclusions and future avenues of study. An appendix is devoted to a detailed derivation of the non-equilibrium Green's functions which are used for computing the expectation values of the relevant observables.

II. THE MODEL

In our subsequent investigations in this article we will work with the linear σ model [11], and furthermore, will take into consideration the electromagnetic interactions of the neutral pion only. The interactions of the charged pions give rise to out of equilibrium processes that produce a single (direct) photon at lowest order in α through spinodal growth of charged pion fluctuations; these processes have recently been studied in [7]. On the other hand, the anomalous interactions of the π^0 will result in the distinctly different process of diphoton production, with the 2 emitted photons being polarized perpendicular to each other and will lead to a polarization asymmetry due to the pseudoscalar nature of the interaction. The Lagrangian density of the model under consideration is given by

$$\begin{aligned} \mathcal{L} = & \frac{1}{2} \partial_\mu \vec{\Phi} \cdot \partial^\mu \vec{\Phi} - \frac{1}{2} m^2(t) \vec{\Phi} \cdot \vec{\Phi} + \lambda (\vec{\Phi} \cdot \vec{\Phi})^2 - h\sigma \\ & - \frac{1}{4} F_{\mu\nu} F^{\mu\nu} + \frac{e^2}{32\pi^2} \pi^0 F_{\mu\nu} \tilde{F}^{\mu\nu} \end{aligned} \quad (2.1)$$

where $\vec{\Phi}$ is an $O(N + 1)$ vector, $\vec{\Phi} = (\sigma, \pi^0, \vec{\pi})$ and $\vec{\pi}$ represents the $N - 1$ pions, $\vec{\pi} = (\pi^1, \pi^2, \pi^3, \dots, \pi^{N-1})$ and $m^2(t)$ introduces quench situation [6] “by hand”. As emphasized in [6] the sudden quench approximation can be generalized to allow a “cooling” relaxation time (of the order of one fm/c) without major qualitative changes in the result and consistent with the numerical results including expansion [4,5].

We then take

$$m^2(t) = \frac{M_\sigma^2}{2} \left[\frac{T_i^2}{T_c^2} \Theta(-t) - 1 \right] \quad T_i > T_c. \quad (2.2)$$

We will also consider below the evolution of the system from a non-equilibrium initial condition at $T_i = 0$ for comparison.

The last term in eq.(2.1) results from the axial anomaly. In a constituent quark model it is known to arise from the quark triangle diagram, which for 3 flavors of quarks leads to the amplitude for π^0 decay into two photons described by the effective interaction vertex in the above Lagrangian [12].

At this point we want to remark that while the nature of the effective Lagrangian for the neutral pion decay into photons is clearly understood *in perturbation theory*, it is by no means clear that this effective interaction also describes strongly out of equilibrium situations. It has been recently pointed out by Pisarski, Tytgat and Baier et. al. [13] that *in equilibrium* and above the critical temperature there is a drastic modification of the anomalous vertices. It is conceivable that the anomalous decay vertices are modified in strongly out of equilibrium situations as well. We are currently studying this possibility in detail within the framework of non-equilibrium field theory in a constituent quark model, but in this article we accept the anomalous vertex determined by the perturbative triangle diagram in equilibrium and study its consequences.

The linear sigma model is at best a phenomenological model, and its parameters are fixed by the low energy phenomenology of pion physics to be [11]:

$$\begin{aligned}
M_\sigma &\approx 600 \text{ MeV} \ ; \ f_\pi \approx 93 \text{ MeV} \ ; \ \lambda \approx 4.5 \\
h &\approx (120 \text{ MeV})^3 \ ; \ T_c \approx 200 \text{ MeV}.
\end{aligned}
\tag{2.3}$$

This value of the critical temperature T_c is a consequence of the parameters of the model and is somewhat larger than the lattice estimates $T_c \approx 150$ MeV. This is a cutoff theory with an ultraviolet cutoff of the order of $\Lambda \approx 1$ GeV. Although we will be dealing with the $O(4)$ model with 3 pions, we will use the large N limit to provide a consistent, non-perturbative framework to study the dynamics. For a clear description of this approximation and its validity, and its applications to a wide variety of non-equilibrium situations we refer the reader to [14,16,17]. Eventually one should set $N = 3$ which is the number of physical pions in the real world and though questions may be raised as to the validity of the large N expansion in this case, it provides a systematic approximation method to study the non-perturbative physics of the sigma model. More importantly perhaps, it is an approximation scheme that preserves energy conservation (in the absence of expansion), implements PCAC and satisfies the Ward identities of chiral symmetry. As a result, the pions in the asymptotic equilibrium state are *exactly* massless in the absence of the explicit symmetry breaking term.

Non-equilibrium quantum field theory requires a path integral representation along a complex contour in time [18,19], with the Lagrangian density along this contour given by

$$\mathcal{L}_{neq} = \mathcal{L}[\Phi^+] - \mathcal{L}[\Phi^-]
\tag{2.4}$$

with the fields Φ^\pm defined along the forward (+) and backward (−) time branches. For further details see references [14,17]. The non-equilibrium equations of motion are obtained via the tadpole method [17]. As mentioned earlier, in the situations of interest to us in this article, both the σ and π^0 fields may acquire expectation values. Accordingly, we first shift σ and π^0 by their expectation values in the non-equilibrium state

$$\sigma(\vec{x}, t) = \phi(t) + \chi(\vec{x}, t) ; \phi(t) = \langle \sigma(\vec{x}, t) \rangle \quad (2.5)$$

$$\pi^0(\vec{x}, t) = \zeta(t) + \psi(\vec{x}, t) ; \zeta(t) = \langle \pi^0(\vec{x}, t) \rangle$$

with the tadpole conditions

$$\langle \chi(\vec{x}, t) \rangle = 0 ; \langle \psi(\vec{x}, t) \rangle = 0 ; \langle \vec{\pi}(\vec{x}, t) \rangle = 0 \quad (2.6)$$

being imposed to all orders in the corresponding expansion. To leading order in $1/N$, the large- N approximation is equivalent to the following Hartree factorization of the quantum fields:

$$\begin{aligned} \chi^4, (\psi^4) &\rightarrow 6\langle \chi^2 \rangle \chi^2 + \text{constant}, (6\langle \psi^2 \rangle \psi^2 + \text{constant}) \\ \chi^3, (\psi^3) &\rightarrow 3\langle \chi^2 \rangle \chi, (3\langle \psi^2 \rangle \psi), \end{aligned} \quad (2.7)$$

$$\begin{aligned} (\vec{\pi} \cdot \vec{\pi})^2 &\rightarrow (2 + \frac{4}{N})\langle \vec{\pi}^2 \rangle \vec{\pi}^2 + \text{constant} \\ \vec{\pi}^2 \chi^2, (\vec{\pi}^2 \psi^2) &\rightarrow \vec{\pi}^2 \langle \chi^2 \rangle + \langle \vec{\pi}^2 \rangle \chi^2, (\vec{\pi}^2 \langle \psi^2 \rangle + \langle \vec{\pi}^2 \rangle \psi^2) \\ \vec{\pi}^2 \chi, (\vec{\pi}^2 \psi) &\rightarrow \langle \vec{\pi}^2 \rangle \chi, (\langle \vec{\pi}^2 \rangle \psi). \end{aligned} \quad (2.8)$$

In addition to the above factorizations, we will implement a further Hartree factorization of the Wess-Zumino term,

$$\psi F \tilde{F} \rightarrow \psi \langle F \tilde{F} \rangle. \quad (2.9)$$

There is no *a priori* justification for the factorization of the anomalous term, but this allows us to treat the full back-reaction problem self-consistently maintaining energy conservation (in the absence of expansion).

To leading order in $1/N$, the effective non-equilibrium Lagrangian density is then given by

$$\begin{aligned} \mathcal{L}[\phi + \chi^+, \vec{\pi}^+] - \mathcal{L}[\phi + \chi^-, \vec{\pi}^-] &= \left\{ \frac{1}{2}(\partial\chi^+)^2 + \frac{1}{2}(\partial\psi^+)^2 + \frac{1}{2}(\partial\vec{\pi}^+)^2 \right. \\ &\quad \left. - \mathcal{V}_1(t)\chi^+ - \mathcal{V}_2(t)\psi^+ + 8\zeta(t)\phi(t)\chi\psi - \frac{1}{2}\mathcal{M}_\chi^{+2}(t)\chi^{+2} - \frac{1}{2}\mathcal{M}_\psi^{+2}(t)\psi^{+2} - \frac{1}{2}\mathcal{M}_{\vec{\pi}}^{+2}(t)\vec{\pi}^{+2} \right\} \\ &\quad - \frac{1}{4}F_{\mu\nu}^+ F^{+\mu\nu} + \frac{e^2}{32\pi^2}\zeta(t)F_{\mu\nu}^+ \tilde{F}^{+\mu\nu} + \frac{e^2}{32\pi^2}\psi^+ \langle F_{\mu\nu}^+ \tilde{F}^{+\mu\nu} \rangle - \{+ \longrightarrow -\}. \end{aligned} \quad (2.10)$$

where

$$\mathcal{V}_1(t) = \ddot{\phi}(t) + \phi(t)[m^2(t) + 4\lambda\phi^2(t) + 4\lambda\zeta^2(t) + \Sigma(t)] - h \quad (2.11)$$

$$\mathcal{V}_2(t) = \ddot{\zeta}(t) + \zeta(t)[m^2(t) + 4\lambda\phi^2(t) + 4\lambda\zeta^2(t) + \Sigma(t)] \quad (2.12)$$

$$\mathcal{M}_\pi^2(t) = m^2(t) + 4\lambda\phi^2(t) + 4\lambda\zeta^2(t) + \Sigma(t) \quad (2.13)$$

$$\mathcal{M}_\chi^2(t) = m^2(t) + 12\lambda\phi^2(t) + 4\lambda\zeta^2(t) + \Sigma(t). \quad (2.14)$$

$$\mathcal{M}_\psi^2(t) = m^2(t) + 12\lambda\zeta^2(t) + 4\lambda\phi^2(t) + \Sigma(t). \quad (2.15)$$

$$\Sigma(t) = 4\lambda \left[\langle \vec{\pi}^2 \rangle(t) - \langle \vec{\pi}^2 \rangle(0) \right] \quad (2.16)$$

The subtraction of $\langle \vec{\pi}^2 \rangle(t)$ at $t = 0$ leads to a renormalization of the mass term given in (2.2) [6]. The presence of the $\chi\psi$ mixing term does not contribute to the dynamics of the theory in the large N limit because such a term is formally of $\mathcal{O}(1/N)$ and is therefore subleading. In the large N limit, the Lagrangian becomes quadratic at the expense of a self-consistency condition for $\Sigma(t)$.

The pion fields obey a linear Heisenberg evolution equation (in terms of the self-consistent field), and the Heisenberg field operators can be expanded as

$$\vec{\pi}(\vec{x}, t) = \frac{1}{\sqrt{\Omega}} \sum_k \frac{1}{\sqrt{2W_{k,i}}} [\vec{a}_k U_k(t) e^{i\vec{k}\cdot\vec{x}} + \vec{a}_k^\dagger U_k^*(t) e^{-i\vec{k}\cdot\vec{x}}] \quad (2.17)$$

where a_k, a_k^\dagger are the destruction and creation operators of Fock states associated with the pion field and Ω is the quantization volume. The frequencies $W_{k,i}$ determine the initial state and will be specified below.

It is found [5,6] that the pion mode functions $U_k(t)$ and the order parameter(s) $\phi(t), \zeta(t)$ obey the following equations of motion

$$\ddot{\phi}(t) + [m^2(t) + 4\lambda\phi^2(t) + 4\lambda\zeta^2(t) + \Sigma(t)]\phi(t) - h = 0 \quad (2.18)$$

$$\ddot{\zeta}(t) + [m^2(t) + 4\lambda\phi^2(t) + 4\lambda\zeta^2(t) + \Sigma(t)]\zeta(t) - \frac{e^2}{32\pi^2}\langle F\tilde{F} \rangle = 0 \quad (2.19)$$

$$\left[\frac{d^2}{dt^2} + k^2 + m^2(t) + 4\lambda\phi^2(t) + 4\lambda\zeta^2(t) + \Sigma(t) \right] U_k(t) = 0 \quad (2.20)$$

At this stage we must specify the initial conditions on the quantum pion fields. We will study the evolution with different sets of initial conditions to determine the sensitivity of the qualitative features of the dynamics to changes in the initial conditions:

1. In the first case we will *assume* that at the initial time (the time of the “quench”) the quantum fluctuations are in local thermodynamic equilibrium at the initial temperature $T_i > T_c$ and that the mode functions $U_k(0)$ correspond to the instantaneous positive frequency modes with mass

$$M^2 = m^2(t < 0) + 4\lambda(\phi^2(0) + \zeta^2(0)). \quad (2.21)$$

In addition, the order parameter is assumed to have a non-zero initial amplitude in the π^0 direction i.e. $\zeta(0) \neq 0$ and $\phi(0) = 0$.

2. In the second scenario we assume that the order parameter is initially displaced from the equilibrium position exactly as in (1), but the modes are chosen to be at zero temperature, $T_i = 0$, so that the $m^2(t < 0) = -\frac{M_\sigma^2}{2}$, and the mass for the modes is

$$M^2 = -\frac{M_\sigma^2}{2} + 4\lambda(\phi^2(0) + \zeta^2(0)). \quad (2.22)$$

However, in both the above cases, the modes must satisfy,

$$U_k(0) = 1; \quad \dot{U}_k(0) = -iW_{k,i} ; \quad W_{k,i} = \sqrt{k^2 + M^2}. \quad (2.23)$$

These initial conditions are to be treated only as assumptions that allow concrete calculations and estimates and are by no means a definitive description of the physics. The correct set of initial conditions should in principle be obtained by evolving parton cascade models well into the regime in which hadronic physics can be described by low energy effective lagrangians. This is certainly an ambitious task and clearly beyond our current understanding. Thus in view of the lack of clear and precise knowledge of the initial conditions, we are restricted to investigating a physically plausible initialization of the dynamics. The above choice is the simplest that allows a concrete calculation and a quantitative description of the dynamics.

With these initial conditions we are led to the self-consistent equation [5,6]

$$\Sigma(t) = (N - 1) \int^{\Lambda} \frac{d^3k}{(2\pi)^3} \frac{|U_k(t)|^2 - 1}{2W_{k,i}} \coth \left[\frac{W_{k,i}}{2T_i} \right]. \quad (2.24)$$

For the initial conditions (2), we must set $T_i = 0$. In addition, the initial conditions on the order parameters and their derivatives, namely $\phi(0)$, $\dot{\phi}(0)$, $\zeta(0)$ and $\dot{\zeta}(0)$ must also be specified. At the moment they are completely arbitrary, constrained only by the requirement that typical energy densities in a DCC region are \sim a few GeV/fm³ (which is the typical energy deposited in the central rapidity region in a heavy-ion collision).

Clearly, a self consistent solution to the above equations will only be possible after understanding the time evolution of the $\langle F\tilde{F} \rangle$ term in (2.19). This in turn, will require an investigation of the $\zeta F\tilde{F}$ interaction in (2.10). As shown below, it will give rise to out of equilibrium photon production via a process of parametric resonance.

III. PHOTON PRODUCTION

Let us now turn to the electromagnetic sector of the theory. Since the processes of interest to us do not involve photons in intermediate states, we can avoid potential gauge ambiguities by working in the Coulomb gauge and restricting our attention to the transverse, physical

degrees of freedom. In this gauge, the quadratic part of the Lagrangian for the physical photons, is given by

$$\mathcal{L}_{em}^q = \frac{1}{2}[\partial_\mu \vec{A}_T]^2 + \frac{e^2}{32\pi^2} \frac{\zeta(t)}{f_\pi} F \tilde{F}. \quad (3.1)$$

Since

$$F \tilde{F} = 8(\partial_0 A_i)(\partial_j A_k) \epsilon^{0ijk} + \text{total divergence} \quad (3.2)$$

\mathcal{L}_{em}^q may be re-written as,

$$\begin{aligned} \mathcal{L}_{em}^q &= \frac{1}{2}[\partial_\mu \vec{A}_T]^2 + \frac{e^2}{4\pi^2} \frac{\zeta(t)}{f_\pi} (\partial_0 A_i)(\partial_j A_k) \epsilon^{0ijk} \\ &= -\frac{1}{2} \vec{A}_T \cdot \square \vec{A}_T - \frac{e^2}{4\pi^2} \frac{\dot{\zeta}(t)}{2f_\pi} A_T^i \partial_j A_T^k \epsilon^{ijk} + \text{total divergence} \end{aligned} \quad (3.3)$$

leading to the Heisenberg operator-equation of motion:

$$\square \vec{A}_T + \frac{e^2}{4\pi^2} \frac{\dot{\zeta}(t)}{f_\pi} \vec{\nabla} \times \vec{A}_T = 0. \quad (3.4)$$

Recall that the interaction term $\psi F \tilde{F}$ has been Hartee-factorized to give $\psi \langle F \tilde{F} \rangle$ and does not contribute to the operator equation of motion above.

The physical content of the equations of motion becomes manifest once we expand the transverse photon field in terms of the circularly polarized states. For a mode with wave vector \vec{k} , consider the triad of vectors \hat{k} , $\vec{\epsilon}_1(\vec{k})$, $\vec{\epsilon}_2(\vec{k})$ with the properties

$$\begin{aligned} \vec{\epsilon}_1(-\vec{k}) &= -\vec{\epsilon}_1(\vec{k}) ; \vec{\epsilon}_2(-\vec{k}) = \vec{\epsilon}_2(\vec{k}) \\ \hat{k} \times \vec{\epsilon}_1(\vec{k}) &= \vec{\epsilon}_2(\vec{k}) ; \hat{k} \times \vec{\epsilon}_2(\vec{k}) = -\vec{\epsilon}_1(\vec{k}). \end{aligned} \quad (3.5)$$

We can now construct the circular polarization vectors

$$\vec{\epsilon}_+(\vec{k}) = \frac{i\vec{\epsilon}_1(\vec{k}) + \vec{\epsilon}_2(\vec{k})}{\sqrt{2}} ; \vec{\epsilon}_-(\vec{k}) = \frac{i\vec{\epsilon}_1(\vec{k}) - \vec{\epsilon}_2(\vec{k})}{\sqrt{2}} \quad (3.6)$$

In terms of these circular polarization vectors we can perform the usual mode expansion for the fields in terms of annihilation and creation operators:

$$\begin{aligned}
\vec{A}_T(\vec{x}, t) &= \frac{1}{\sqrt{\Omega}} \sum_{\vec{k}} \vec{A}_T(\vec{k}, t) \\
&= \frac{1}{\sqrt{\Omega}} \sum_{\vec{k}} \frac{1}{\sqrt{2k}} \left\{ [b_+(\vec{k})V_{1\vec{k}}(t)\vec{\epsilon}_+(\vec{k}) + b_-(\vec{k})V_{2\vec{k}}(t)\vec{\epsilon}_-(\vec{k})] e^{i\vec{k}\cdot\vec{x}} + \text{h.c.} \right\}
\end{aligned} \tag{3.7}$$

We find that the mode functions obey the following equations of motion

$$\frac{d^2 V_{1k}}{dt^2} + k^2 V_{1k}(t) - k \frac{e^2}{4\pi^2} \frac{\dot{\zeta}(t)}{f_\pi} V_{1k} = 0 \tag{3.8}$$

$$\frac{d^2 V_{2k}}{dt^2} + k^2 V_{2k}(t) + k \frac{e^2}{4\pi^2} \frac{\dot{\zeta}(t)}{f_\pi} V_{2k} = 0. \tag{3.9}$$

To these equations of motion we must append initial conditions. Now, we want to describe the process of emission of physical, circularly polarized massless photons. Therefore the initial conditions for these mode functions must be:

$$V_{1,2k}(0) = 1 \quad , \quad \dot{V}_{1,2k}(0) = -ik. \tag{3.10}$$

Furthermore, we will assume that at the initial time, the photons are in local thermodynamic equilibrium at the initial temperature. We will also study the case in which there are no initial photons by taking the initial temperature of the photon distribution function to zero.

There are several noteworthy features of these equations of motion that deserve comment:

1. The zero mode of the neutral pion field acts as time dependent mass term (with a momentum dependence), which will result in a “squeezing” of the quantum fields.
2. The equations decouple when written in terms of the *circular polarization* mode functions.
3. The effective “mass terms” for the two polarizations have opposite signs. These last two features are a direct consequence of the pseudoscalar nature of the coupling of the neutral pion to the vector field.

As the π^0 zero mode executes quasiperiodic oscillations, the solutions to the mode equations (3.8,3.9) will display the phenomenon of parametric resonance, for some values of k . In other words, for certain (forbidden) bands of values in k -space, the modes will grow exponentially with Floquet-like solutions. This growth of modes will be reflected in the exponential growth of particle number (in this case, the number of asymptotic photons). Furthermore, since the coupling affects right and left handed polarizations differently, there will be a polarization asymmetry in the photon emission. A quantitative analysis of this phenomenon will require a solution of the coupled differential equations (2.18), (2.19), (2.20), (2.24) and (3.8, 3.9) which will be done numerically below.

The number operator for asymptotic photons is given by [7]:

$$N(k, t) = \frac{1}{2k} \left[\dot{\vec{A}}_T(\vec{k}, t) \cdot \dot{\vec{A}}_T(-\vec{k}, t) + k^2 \vec{A}_T(\vec{k}, t) \cdot \vec{A}_T(-\vec{k}, t) \right] - 1 \quad (3.11)$$

In order to obtain the expectation value of this Heisenberg operator in the initial density matrix, one needs the quantum two-point functions for the theory. These can be obtained from the expansion (3.8). A detailed derivation of these correlators in terms of non-equilibrium Green's functions has been given in an appendix. From the expressions for the Wightman functions (A18) and (A19) it is easy to see that the expectation value of the number operator in terms of the mode functions (3.8,3.9), has the following form,

$$\begin{aligned} \langle N_k(t) \rangle &= \frac{1}{4k^2} \coth \left[\frac{k}{2T_i} \right] \left[|\dot{V}_{1k}(t)|^2 + k^2 |V_{1k}(t)|^2 \right] - \frac{1}{2} + \\ &\quad \frac{1}{4k^2} \coth \left[\frac{k}{2T_i} \right] \left[|\dot{V}_{2k}(t)|^2 + k^2 |V_{2k}(t)|^2 \right] - \frac{1}{2} \\ &\equiv N_+(k, t) + N_-(k, t) \end{aligned} \quad (3.12)$$

Only the symmetric part of the Green's functions contribute to the expectation value. From this expression for the number of asymptotic, transverse, massless photons produced, and the evolution equations (3.8,3.9) it is clear that the number of left and right circularly polarized photons produced by the evolution of the zero mode of the neutral pion field will in general

be different, since the evolution of the modes are different. The polarization asymmetry in the photons produced may be an experimentally relevant signal. We define this asymmetry as

$$\Xi(k, t) = \frac{(N_+(k, t) - N_-(k, t))}{(N_+(k, t) + N_-(k, t))}. \quad (3.13)$$

The dynamics of the process of photon production via the non-equilibrium evolution of the expectation value of the neutral pion field is then obtained by solving the self-consistent set of equations of motion (2.18,2.19,2.20,2.24, 3.8,3.9) with the initial conditions (2.23, 3.10).

IV. NUMERICAL ANALYSIS

It is convenient to work with dimensionless variables for purposes of numerical analysis. The relevant dimensionful scale in this problem is $\Lambda_{QCD} \sim 200 \text{ MeV} = M_F$, and we use it to scale out the dimensions of all the relevant variables in the equations of motion:

$$\xi(t) = \frac{\zeta(t)}{M_F}, \quad \tau = M_F t, \quad \eta = \frac{\phi}{M_F}, \quad q = \frac{k}{M_F}, \quad \omega_q = \sqrt{q^2 + \frac{M^2}{M_F^2}} \quad (4.1)$$

$$\mathcal{U}_q(t) = \frac{U_k(t)}{\sqrt{\omega_q}}, \quad \mathcal{U}_q(0) = \frac{1}{\sqrt{\omega_q}}, \quad \frac{d\mathcal{U}_q}{d\tau}(0) = -i\sqrt{\omega_q} \quad (4.2)$$

$$\chi_{1,2q}(t) = \frac{V_{1,2k}(t)}{\sqrt{q}}, \quad \chi_{1,2q}(0) = \frac{1}{\sqrt{q}}, \quad \frac{d\chi_{1,2q}}{d\tau}(0) = -i\sqrt{q} \quad (4.3)$$

$$H = \frac{h}{M_F^3} \approx 0.22, \quad \frac{\Lambda}{M_F} = 5, \quad r = \frac{T_i}{M_F}. \quad (4.4)$$

Thus the Wronskian condition for the mode functions defined in terms of dimensionless variables is

$$\frac{d\chi_{1,2q}}{d\tau}\chi_{1,2q}^* - \frac{d\chi_{1,2q}^*}{d\tau}\chi_{1,2q} = -2i. \quad (4.5)$$

The expectation value of the anomaly term which appears in the equations of motion can now be obtained as follows

$$\begin{aligned}\langle F\tilde{F} \rangle &= 8\langle \partial_0 A_T^i \partial_j A_T^k \rangle \epsilon^{ijk} \\ &= 8 \frac{d}{dt} \int \frac{d^3 k}{(2\pi)^3} \int \frac{d^3 k'}{(2\pi)^3} e^{-i(\vec{k}+\vec{k}')\cdot\vec{x}} \langle A_T^i(\vec{k}, t) A_T^l(\vec{k}', t') \rangle (-ik'_j) \epsilon^{ijl} |_{t=t'}.\end{aligned}\quad (4.6)$$

The two point correlator in the above expression can be obtained from the coincidence limit of the Green's functions of the full quantum theory, given in eqs. (A18) and (A19). In this case, only the antisymmetric part of the Green's function contributes to the expectation value. The expectation of $F\tilde{F}$ in the initial density matrix, is then found to be:

$$\langle F\tilde{F} \rangle = \frac{M_F^4}{\pi^2} \int q^3 dq \coth \left[\frac{q}{2r} \right] \frac{d}{d\tau} (|\chi_{2q}|^2 - |\chi_{1q}|^2) \quad (4.7)$$

where q is the dimensionless momentum and use was made of the Wronskian condition (4.5).

The full dynamics of the system can now be followed by numerically solving the following set of equations:

$$\frac{d^2 \eta(\tau)}{d\tau^2} + \frac{m^2(\tau)}{M_F^2} + 4\lambda\eta(\tau)[\eta^2(\tau) + \xi^2(\tau) + \Sigma(\tau)] - H = 0, \quad (4.8)$$

$$\frac{d^2 \xi(\tau)}{d\tau^2} + \frac{m^2(\tau)}{M_F^2} \xi(\tau) + 4\lambda\xi(\tau) [\eta^2(\tau) + \xi^2(\tau) + \Sigma(\tau)] - \Gamma(\tau) = 0$$

$$\frac{d^2 \mathcal{U}_q}{d\tau^2} + \left(q^2 + \frac{m^2(\tau)}{M_F^2} + 4\lambda\eta^2(\tau) + 4\lambda\xi^2(\tau) + 4\lambda\Sigma(\tau) \right) \mathcal{U}_q(\tau) = 0$$

$$\frac{d^2 \chi_{1q}}{d\tau^2} + \left(q^2 - \frac{\alpha M_F}{\pi f_\pi} q \frac{d\xi}{d\tau} \right) \chi_{1q} = 0$$

$$\frac{d^2 \chi_{2q}}{d\tau^2} + \left(q^2 + \frac{\alpha M_F}{\pi f_\pi} q \frac{d\xi}{d\tau} \right) \chi_{2q} = 0$$

with the initial conditions

$$\mathcal{U}_q(0) = \frac{1}{\sqrt{\omega_q}}, \quad \dot{\mathcal{U}}_q(0) = -i\sqrt{\omega_q} \quad (4.9)$$

$$\chi_{1,2q}(0) = \frac{1}{\sqrt{q}}, \quad \dot{\chi}_{1,2q}(0) = -i\sqrt{q}$$

and the self-consistent fluctuations given by

$$\Sigma(\tau) = \frac{2}{4\pi^2} \int_0^5 q^2 dq (|\mathcal{U}_q(\tau)|^2 - |\mathcal{U}_q(0)|^2) \coth \left[\frac{\omega_q}{2r} \right] \quad (4.10)$$

$$\Gamma(\tau) = \frac{\alpha M_F}{8\pi^3 f_\pi} \int_0^5 q^3 dq \coth \left[\frac{q}{2r} \right] \frac{d}{d\tau} (|\chi_{2q}|^2 - |\chi_{1q}|^2)$$

The number of photons per unit volume per unit phase space is then

$$\begin{aligned} (2\pi)^3 \frac{d(\langle N_q(\tau) \rangle - \langle N_q(0) \rangle) / \Omega}{d^3q} &\equiv \frac{n(q, \tau)}{|q|} \\ &= \frac{1}{4q} \coth \left[\frac{q}{2r} \right] \left[\left| \frac{d\chi_{1q}}{d\tau} \right|^2 + \left| \frac{d\chi_{2q}}{d\tau} \right|^2 + q^2 (|\chi_{1q}|^2 + |\chi_{2q}|^2) - 4q \right] \end{aligned} \quad (4.11)$$

Here, we have taken the continuum limit, and subtracted out the number of photons present at $t = 0$ which forms a thermal background at the initial temperature T_i . We have also introduced the quantity $n(q, \tau) = (2\pi)^3 |q| \frac{d(\langle N_q(\tau) \rangle - \langle N_q(0) \rangle) / \Omega}{d^3q}$. Our numerical results for the photon spectrum and the invariant rate will be expressed in terms of this quantity. The invariant rate for photon production can be obtained by looking at the time derivative of (4.11) and using the mode equations, it is found to be:

$$(2\pi^3) \frac{d(\langle \dot{N}(\tau) \rangle / \Omega)}{d^3q} = \frac{\alpha M_F}{4\pi f_\pi} \xi \coth \left[\frac{q}{2r} \right] \frac{d}{d\tau} [|\chi_{1q}|^2 - |\chi_{2q}|^2]. \quad (4.12)$$

A comparison of this expression for the rate and that for the expectation value of the anomaly term in eq.(4.7) clearly indicates the the important role played by the latter quantity in ensuring energy conservation. The photons produced lead to a non-zero expectation value for $F\tilde{F}$ which then feeds back into the equation of motion for the zero mode.

The above expression for the rate will also turn out to be useful for obtaining quantitative estimates of the location of the unstable bands. In equilibrium, $|\chi_{1q}|^2 = |\chi_{2q}|^2 = 1/q$, and thus the rate vanishes. However, out of equilibrium and particularly for the processes that we have considered here, both $|\chi_{1q}|$ and $|\chi_{2q}|$ will acquire small time dependent modulations around a mean value, with a frequency that is roughly $\sim q$, since that is the relevant scale in the problem. Thus the oscillation frequency of $\frac{d}{d\tau}(|\chi_{1q}|^2 - |\chi_{2q}|^2)$ is $\sim 2q$. Now the maximum buildup of particles will occur when this oscillation is in phase with the derivative of the zero mode $\dot{\xi}(\tau)$, resulting in a positive rate for all times, causing a resonant production of photons. Therefore the unstable bands will be determined by the condition

$$q_{res}M_F = k_{res} \approx \frac{\omega_{\pi^0}}{2}. \quad (4.13)$$

with ω_{π^0} being the oscillation frequency of the expectation value of the π^0 component of the order parameter. For small oscillations in the π^0 direction, $\omega_{\pi^0} = M_\pi = 140$ MeV and so the resonant band should be at $k = 70$ MeV, which is exactly the energy of two back to back photons produced by a π^0 at rest. The validity of these qualitative arguments and particularly that of eq. (4.13) will be borne out by the results of the numerical analysis which we present below.

For all the cases that we considered, we chose to represent the “quench” from an initial temperature $T_i = 1.1T_c = 220$ MeV to zero temperature, and we tracked the evolution of the system up to a time of about 10 fm/c which is the typical time scale after which the effects of hydrodynamical expansion become important. Since we are interested in studying the optimal situation for large anomalous photon production from the non-equilibrium evolution of the neutral pion, we have performed our numerical analysis in all cases with the initial value of the σ component as well as its initial time derivative being zero. An initial condition with both the neutral pion and σ components being different from zero will result in a smaller photon yield. This is because, for a given initial energy density, if the σ component is large,

the π^0 component must be smaller and it is the π^0 zero mode that drives the parametric amplification. Furthermore since the sigma model is an effective theory below 1 GeV we look only at photons with momenta less than this value. Photons with energy larger than a GeV will be indistinguishable from the hard photon background and much less significant as a signature of low p_T physics associated with DCC's or the chiral phase transition.

Results:

The results of the numerical calculations are shown in figures (1) through (6). We first look at the result obtained for small oscillations in the π^0 direction with initial conditions $\zeta(0) = \xi(0)M_F = 0.1M_F$, $\dot{\xi}(0) = 0$, $\phi(0) = \dot{\phi}(0) = 0$. This is the perturbative regime, in which $\xi(\tau)$ undergoes small amplitude (almost undamped) oscillations, with emission of back to back photons at 70 MeV. Fig.(1) shows the spectrum of photons emitted per unit volume, $n(q, \tau) = (2\pi)^3|q|\frac{d(N(\tau)-N(0))/\Omega}{d^3q}$, (in units of fm^{-1}) at time $t = 10 \text{ fm}/c$, for the small amplitude initial conditions described above. Here, we have subtracted out the thermal distribution of photons that are present initially at $t = 0$ when the system is in equilibrium at a temperature, $T_i = 220 \text{ MeV}$. Clearly, there is a resonant peak which upon closer inspection is found to be exactly centered around 70 MeV. This corresponds to the usual perturbative decay of zero momentum pions and as expected, the peak value of the photon number, 2.75×10^{-5} , is $\mathcal{O}(\alpha^2)$. In this perturbative (small amplitude) regime the location of the unstable band for small oscillations can be easily obtained by solving the mode equations (3.8,3.9) assuming a sinusoidal time dependence for the zero mode, which leads to a Mathieu equation for the non-zero modes for which the position of the unstable bands can be found in textbooks [20].

Figs.(2.a) and (2.b) show $\dot{\xi}(\tau)$ and $n(q, \tau) = (2\pi)^3|q|\frac{d(N(\tau)-N(0))/\Omega}{d^3q}$, (in units of fm^{-1}) at time $t = 10 \text{ fm}/c$ respectively, for the initial conditions $\zeta(0) = \xi(0)M_F = 1.0M_F$, $\dot{\xi}(0) = 0$, $\phi(0) = \dot{\phi}(0) = 0$. This corresponds to preparing a configuration with an energy density $\lambda(\zeta(0)^2 - f_\pi^2)^2 \approx 0.5 \text{ GeV}/\text{fm}^3$ above the thermal energy density. $\dot{\xi}$ now evolves with a larger

amplitude and also a higher frequency as shown in Figure (2.a). The small damping has its origins in mode mixing and excitations of the quantum fluctuations (pions and “sigmas”) via spinodal and parametric amplification, and also to a smaller extent, the contribution from photon production. The spectrum of emitted photons is shown in Fig.(2.b). It features a prominent peak centered around 306 MeV with a much larger value, 0.005 fm^{-1} (vs. $0.0000275 \text{ fm}^{-1}$ in Fig.(1)) which is of $\mathcal{O}(\alpha)$ (rather than $\mathcal{O}(\alpha^2)$ as in Fig.(1)) showing explicitly the non-perturbative nature of the amplification phenomenon. The band is also quite broad with a width $\approx 120 \text{ MeV}$. This is clearly a non-perturbative effect caused by parametric resonance. In fact our qualitative argument (4.13) for obtaining the resonant frequency works rather well here. ω_{π^0} can be read off from the oscillations of the zero mode in Figure (2.a) and is $\approx \frac{2\pi}{2} \times 200 \text{ MeV}$ so that $k_{res} \approx \omega_{\pi^0}/2 \approx 310 \text{ MeV}$. To illustrate the point of parametric amplification, Fig.(2.c) shows the invariant rate $\dot{n}(q, \tau) = (2\pi)^3 |q| \frac{d\dot{N}(\tau)/\Omega}{d^3q}$, (in units of fm^{-2}) for q at the center of the resonant band $k = k_{res}$ as a function of time (in units of fm/c). It is important to remark that unlike the small amplitude regime, in this large amplitude case, the rate is $\mathcal{O}(\alpha)$ rather than the perturbative result $\mathcal{O}(\alpha^2)$. This figure clearly displays a *positive* quasiperiodic solution with a growing envelope (the “true” invariant rate should be obtained by dividing by the total number of photons as a function of time, as the above rate has been defined as the time derivative of the number of photons, not of its logarithm). Our numerical studies show that, away from the center of the resonant band, the rate samples negative values also, thus leading to a lower photon yield for q values away from the center.

With a larger initial amplitude for the π^0 zero mode, we see the same non-perturbative effects as before with a much larger enhancement. Figs.(3.a), (3.b) and (3.c) show the results for initial conditions $\zeta(0) = \xi(0)M_F = 2.0M_F$, $\dot{\xi}(0) = 0$, $\phi(0) = \dot{\phi}(0) = 0$. The energy density corresponding to this initial state is $\approx 12 \text{ GeV}/\text{fm}^3$. It is not surprising that for such a large energy density, the peak in the photon spectrum (Fig.(3.b)) and the invariant

rate at the resonant frequency (Fig.(3.c)) are about an order of magnitude larger than the previous case. Furthermore the position of the peak is now shifted further to the right to 625 MeV in qualitative agreement with the argument (4.13).

As anticipated in the discussions of the previous section, these non-perturbative effects and the pseudoscalar nature of the interaction, will give rise to a polarization asymmetry in the photons produced, as well as a non-equilibrium expectation value for $F\tilde{F}$.

In Figures (4.a) and (4.b) we show the polarization asymmetry at the resonant value of q ; $\Xi(q_{res}, \tau) = (n_+(q_{res}, \tau) - n_-(q_{res}, \tau))/(n_+(q_{res}, \tau) + n_-(q_{res}, \tau))$ as a function of time for $k = 306$ MeV, $\xi(0) = 1.0$ (corresponding to the initial conditions of Figs.(2)) and $k = 625$ MeV, $\xi(0) = 2.0$ (corresponding to Figs.(3)). Although this asymmetry is a (quasi) oscillatory function of time, the average over a time scale of about 10 fm/c, yields an estimate of $|\Xi(q_{res}, t)| = 0.05 - 0.10$ for the values used in the figures.

The behaviour of $\Gamma(\tau) = \alpha M_F \langle F\tilde{F} \rangle / 8\pi f_\pi$ (in units of M_F^4) as a function of time up to 10 fm/c is shown in Figures (5.a) and (5.b). Though the behaviour is oscillatory, it is not symmetric about zero and is of order $10^{-4} - 10^{-3} M_F^4$. Thus $\langle F\tilde{F} \rangle$ itself is of order $0.1 - 1 M_F^4$.

We have also studied non-equilibrium initial conditions that do not correspond to local thermodynamic equilibrium by setting T_i to zero, in the initial conditions and relevant quantities.

Fig.(6.a) shows $n(q, \tau) = (2\pi)^3 |q| \frac{d(N(\tau) - N(0))/\Omega}{d^3q}$, (in units of fm^{-1}) at time $t = 10$ fm/c respectively, for the initial conditions $\zeta(0) = \xi(0)M_F = 1.0M_F$, $\dot{\xi}(0) = 0$, $\phi(0) = \dot{\phi}(0) = 0$, $T_i = 0$. Comparing this figure with Fig.(2.b) we see that the main features are qualitatively the same. The amplitude is smaller in Fig.(6.a), reflecting the Bose-enhancement for $T_i \neq 0$ in Fig.(2.b). There is also a slight shift in the center of the unstable band. In Fig.(6.a) the peak is at $k = 284\text{MeV}$ rather than at $k = 306\text{MeV}$ as in Fig.(2.b). Fig.(6.b) shows the invariant rate $\dot{n}(q, \tau) = (2\pi)^3 |q| \frac{d\dot{N}(t)/\Omega}{d^3q}$, (in units of fm^{-2}) for q at the center of the resonant

band $k = k_{res}$ as a function of time (in units of fm/c) for the same initial conditions as for Fig.(6.a). Fig.(6.c) shows the polarization asymmetry for the same initial conditions.

Clearly the effect is fairly robust in that it mainly depends on the non-equilibrium aspects of the evolution with a rather small quantitative change due to Bose-enhancement if the initial state is in LTE at $T_i \neq 0$. A similar conclusion is obtained after numerical analysis with the initial conditions of Figs.(3.a-c) and $T_i = 0$, with the same qualitative features modified slightly by Bose-enhancement (or the lack thereof).

V. POSSIBLE EXPERIMENTAL SIGNATURES:

In a heavy-ion collision one of the most important contributions to the production of low energy photons is from the anomalous single particle decay of the neutral pion. The neutral pions formed during the hadronization and chiral symmetry breaking stages will mainly decay at freeze out, since their lifetimes (at rest) are $\approx 10^7$ fm/c.

The mechanisms studied above are effective *only* during the typical time scales for the non-equilibrium effects and for large initial amplitudes of the neutral pion component of the order parameter. Numerical estimates of the expansion time scales in the semiclassical [4] and quantum large N approximations within the sigma model [5] reveal a longitudinal expansion time scale between 5 to 10 fm/c (spherical expansion scales are somewhat shorter). Although we have not incorporated expansion in our studies, it is a plausible assumption that even if the initial amplitude for the neutral pion component is large, giving rise to the non-perturbative parametric amplification phenomena described above, this amplitude will have diminished substantially by the end of the expansion stage. Thus most of the non-equilibrium, non-perturbative phenomena will take place *during* the initial stages for a time-scale of about 10 fm/c. Only the photons produced during this non-equilibrium stage will feature the abnormal distributions studied above, whereas the photons emitted via the

perturbative (small amplitude) decay of the neutral pion after freeze out will have the typical distribution with a peak at 70 MeV for decay at rest.

Therefore an experimentally meaningful quantity is the ratio of the total number of photons produced during the non-equilibrium stages with abnormal (parametrically amplified) distributions to half the initial number of π^0 's. Notice that this *assumes* that *all* the π^0 's produced will decay perturbatively to 2 photons. Thus this ratio gives a conservative estimate of the experimental relevance of the abnormal electromagnetic signal and provides an estimate for the experimental signature of the non-equilibrium aspects of anomalous photon production during the chiral phase transition.

We found numerically that the pion number density produced via parametric amplification and spinodal instabilities during the non-equilibrium stages, including the pions present in the thermal bath is about $0.6/\text{fm}^3$ for $\zeta(0) = \xi(0)M_F = 1.0M_F$; and $\approx 5/\text{fm}^3$ for $\zeta(0) = \xi(0)M_F = 2.0M_F$, where $M_F = 200$ MeV. The corresponding numbers for the photons produced by parametric amplification out of equilibrium are $0.0015/\text{fm}^3$ and $0.005/\text{fm}^3$ respectively.

Thus the ratio of the number of amplified photons to the number of decay photons is $\approx 0.1 - 0.2\%$, a rather small number. If the detector can measure final state polarization of photons, this signal must be correlated with the total (integrated over the lifetime of the “fireball”) polarization asymmetry $\Xi_{tot} = |n_+ - n_-|/(n_+ + n_-) \approx 0.05 - 0.1$ where the sum in the denominator refers to the parametrically amplified photons.

Therefore the experimental signature of these non-equilibrium effects resulting in an enhancement of photons produced through the non-equilibrium decay of the neutral pion, will be a peak at momenta $k \geq 300$ MeV with an amplitude less than a percent of the amplitude of the usual π^0 peak and with a polarization asymmetry between 5–10%. (Recall, however that we have assumed that all the neutral pions produced will contribute to the 70 MeV peak by decaying at rest, to two photons.) The photon energy corresponding to the

center of the peak increases with the initial energy density at the onset of the non-equilibrium stage.

Clearly these are small effects leading to less than 1 percent signal over background relative to the usual π^0 peak. However, our estimate is only a lower bound and the effect could still be within the limits of resolution of the detectors and could potentially provide one of the electromagnetic signatures of DCC's.

In the energy region $k \geq 280$ MeV (corresponding to an initial value of $\langle \pi^0 \rangle \approx 200$ MeV) the most problematic interference for detection is the decay of the η pseudoscalar meson into two photons, with a branching ratio of about 40%. This neutral mode of decay for the η meson has the same features as that of the neutral pion, insofar as angular distribution and polarization asymmetry are concerned. We can provide a rough (albeit naive) estimate of the number of diphotons produced by η decay by assuming that the η 's are in equilibrium at the initial temperature since they would not undergo parametric or spinodal amplification; this yields an η number density of about $0.088/\text{fm}^3$. This in turn leads to about $0.035/\text{fm}^3$ diphotons at an energy ≈ 275 MeV. Thus if the initial condition corresponds to a disorientation in the π^0 direction with an expectation value of the neutral pion field ≈ 200 MeV, this would translate to a peak in the photon spectrum in the vicinity of the peak associated with the η meson with about 5% ratio of the peak values. Clearly this is *not* a generic initial condition; for larger values of the π^0 component, the peaks in the distribution will move to larger values of the momenta and their amplitude will be enhanced. Although one could argue that for larger values of the momenta the background photon production from higher mass resonance decays will be important, these will be suppressed by thermal factors and smaller branching ratios.

VI. CONCLUSIONS AND FURTHER QUESTIONS

In this article we have focussed on the study of photon production enhancement through the non-equilibrium stages of relaxation of a DCC via the $U_A(1)$ anomaly.

The premise of the study is that if during a heavy-ion collision a state of large energy density is formed in which the chiral order parameter is “disoriented” with a large amplitude in the π^0 direction, such a state will relax via parametric and spinodal amplifications and will also lead to an enhanced production of photons through the $U_A(1)$ anomaly.

We have studied the optimal situation in which the order parameter has the largest amplitude along the neutral pion direction, with typical amplitudes for the zero mode of the neutral pion $\langle\pi^0\rangle = 200 - 400$ MeV corresponding to energy densities in the initial state between $1 - 10$ GeV/fm³. We have followed the evolution during a “quenched” phase transition from an initial state in local thermodynamic equilibrium at a temperature slightly above the critical temperature, cooled instantaneously to zero temperature, as well as from a non-equilibrium initial condition at $T_i = 0$.

We found that the oscillations of the large amplitude neutral pion lead to parametric amplification of circularly polarized photons resulting in unstable k -bands within which the photon mode functions grow almost exponentially leading to a distinct distribution of the produced photons. The peak of the distribution is correlated with the initial amplitude of the neutral pion component of the order parameter and the initial energy density. This is a non-perturbative phenomenon as clearly seen in the ratio of the amplitudes of the photon distribution functions at the peak between the small amplitude (perturbative) and the large amplitude (non-perturbative) regime.

For initial conditions in which the order parameter has a component only along the π_0 direction, we found that the peak in the photon spectrum moves continuously with the initial amplitude of the π^0 , from $k \approx 300$ MeV for $\langle\pi^0\rangle = 200$ MeV corresponding to an

initial energy density $\approx 1 \text{ GeV}/\text{fm}^3$, to $k \approx 620 \text{ MeV}$ for $\langle \pi^0 \rangle = 400 \text{ MeV}$ corresponding to an initial energy density $\approx 12 \text{ GeV}/\text{fm}^3$ during a time scale of $10 \text{ fm}/c$. The pseudoscalar nature of the interaction results in a net polarization asymmetry of the final state photons which ranges between $0.05 - 0.1$ for the above initial conditions. Both the total number of photons created during this process and their polarization asymmetry are correlated with a non-equilibrium expectation value of the anomaly term $F\tilde{F}$.

These novel distributions for photons produced by the “anomalous” decay result in peaks in the photon spectrum whose ratio to the normal peak resulting from the “perturbative” neutral pion decay at 70 MeV is less than the one percent level. Experimentally this is a rather small signal, but perhaps when correlated with the polarization asymmetry, it may result in an unambiguous signal for non-equilibrium processes during the chiral phase transition.

We believe that these results are fairly encouraging and justify a deeper study of these “anomalous non-equilibrium effects”. The next step in the program is to extend the investigation of reference [13] to understand the effective anomalous vertex out of equilibrium. We plan to study this, within the framework of a constituent quark model or alternatively a NJL model in which the triangle diagram out of equilibrium should furnish the effective vertex for neutral pion decay. After a thorough understanding of the effective $\pi^0 \rightarrow 2\gamma$ vertex and its translation to an effective mesonic theory, we will include hydrodynamic expansion by describing the dynamics in terms of boost invariant variables as in [5].

ACKNOWLEDGMENTS

D.B. and S.P.K. thank B. Mueller for enlightening discussions. D.B. thanks J. D. Bjorken, R. Pisarski, J. Randrup, V. Koch, X. N. Wang, E. Engels and R. Willey for illuminating conversations and suggestions and acknowledges support from N.S.F. through Grant: PHY-

APPENDIX A: DERIVATION OF NON-EQUILIBRIUM GREEN'S FUNCTIONS:

In this appendix we present a complete derivation of the non-equilibrium Green's functions which are needed primarily for the computation of the expectation values of observables, such as the photon number density, and $F\tilde{F}$.

The Lagrangian density given by eqn. (3.4) can be written as

$$-\frac{1}{2}A_T^m \left[\delta^{mn} \square + \frac{e^2}{4\pi^2} \frac{\dot{\zeta}(t)}{f_\pi} \partial_j \epsilon^{mjn} \right] A_T^n + \text{total divergence.} \quad (\text{A1})$$

We now define the Fourier transform of the vector potential as,

$$A_T^m(\vec{x}) = \int \frac{d^3k}{(2\pi)^3} e^{-i\vec{k}\cdot\vec{x}} A_T^m(\vec{k}). \quad (\text{A2})$$

Therefore

$$S_{em} = \int dt \frac{d^3k}{(2\pi)^3} \left\{ -\frac{1}{2} A_T^m(\vec{k}) \left[\delta^{mn} \left(\frac{d^2}{dt^2} + k^2 \right) + i \frac{e^2}{4\pi^2} \frac{\dot{\zeta}(t)}{f_\pi} \epsilon^{mjn} k_j \right] A_T^{*n}(\vec{k}) \right\}. \quad (\text{A3})$$

It also turns out to be convenient to express all our equations in terms of the two operators,

$$P^{mn} = \left(\delta^{mn} - \frac{k^m k^n}{k^2} \right), \quad f^{mn} = \epsilon^{mjn} \frac{k^j}{k}, \quad (\text{A4})$$

where $k = \sqrt{k^j k^j}$ and P^{mn} is the projector onto transverse states. It can be easily verified that these operators have the following properties:

$$P^{mn} f^{nl} = f^{ml}, \quad f^{mn} f^{nl} = -P^{ml}. \quad (\text{A5})$$

The action for the electromagnetic sector is then,

$$\begin{aligned} S_{em} &= \int dt \frac{d^3k}{(2\pi)^3} \left\{ -\frac{1}{2} A_T^i(\vec{k}) P^{im} \left[\delta^{mn} \left(\frac{d^2}{dt^2} + k^2 \right) + ik \frac{e^2}{4\pi^2} \frac{\dot{\zeta}(t)}{f_\pi} f^{mn} \right] P^{jn} A_T^{*j}(\vec{k}) \right\} \\ &= \int dt \frac{d^3k}{(2\pi)^3} \left\{ -\frac{1}{2} A_T^i(\vec{k}) \left[P^{ij} \left(\frac{d^2}{dt^2} + k^2 \right) + ik \frac{e^2}{4\pi^2} \frac{\dot{\zeta}(t)}{f_\pi} f^{ij} \right] A_T^{*j}(\vec{k}) \right\}. \end{aligned} \quad (\text{A6})$$

This is simply a quadratic action for two coupled complex scalar fields. The time dependent mixing term, driven by the coherent oscillations of the neutral pion zero mode $\zeta(t)$, acts like a squeeze parameter. One can decouple the fields, either at the level of the action by diagonalizing the quadratic form, or by rewriting the equations of motion in terms of the appropriate degrees of freedom. We will adopt the latter method. In any case, the problem is completely solved once we obtain all the relevant non-equilibrium two-point functions of the theory. The Green's functions \mathcal{G}_{ij} for the operator appearing in the quadratic action must satisfy:

$$\mathcal{D}_{ij}\mathcal{G}_{jk}(t, t') = -P_{ik}\delta(t - t') \quad (\text{A7})$$

where

$$\mathcal{D}_{ij} = \left\{ P_{ij} \left(\frac{d^2}{dt^2} + k^2 \right) + ik \frac{e^2}{4\pi^2} f_{ij} \frac{\dot{\zeta}(t)}{f_\pi} \right\}. \quad (\text{A8})$$

The Green's function can be expressed in terms of the two linearly independent operators defined in (A4) as

$$\mathcal{G}_{jk}(t, t') = C(t, t')P_{jk} + D(t, t')f_{jk}. \quad (\text{A9})$$

Substituting this into eq. (A7), and equating the symmetric and antisymmetric parts of the two sides of the equation, we find:

$$\begin{aligned} \frac{d^2 C}{dt^2} + k^2 C - ik \frac{e^2}{4\pi^2} \frac{\dot{\zeta}(t)}{f_\pi} D &= -\delta(t - t') \\ \frac{d^2 D}{dt^2} + k^2 D + ik \frac{e^2}{4\pi^2} \frac{\dot{\zeta}(t)}{f_\pi} C &= 0. \end{aligned} \quad (\text{A10})$$

These two differential equations can be decoupled by defining the functions

$$G_1(t, t') = C + iD, \quad G_2(t, t') = C - iD, \quad (\text{A11})$$

which then yields

$$\begin{aligned}\frac{d^2 G_1}{dt^2} + k^2 G_1 - k \frac{e^2}{4\pi^2} \frac{\dot{\zeta}(t)}{f_\pi} G_1 &= -\delta(t-t') \\ \frac{d^2 G_2}{dt^2} + k^2 G_2 + k \frac{e^2}{4\pi^2} \frac{\dot{\zeta}(t)}{f_\pi} G_2 &= -\delta(t-t').\end{aligned}\tag{A12}$$

Also,

$$\mathcal{G}_{jk}(t, t') = \left[\frac{G_1 + G_2}{2} P_{jk} + \frac{G_1 - G_2}{2i} f_{jk} \right].\tag{A13}$$

G_1 and G_2 now satisfy the simple Green's function equations (A12) and can be readily expanded in terms of the mode functions (3.8,3.9) as,

$$\begin{aligned}G_{1,2}(t, t') &= \left[A_{1,2}^> V_{1,2}(t) V_{1,2}^*(t') + B_{1,2}^> V_{1,2}^*(t) V_{1,2}(t') \right] \Theta(t-t') \\ &+ \left[A_{1,2}^< V_{1,2}^*(t) V_{1,2}(t') + B_{1,2}^< V_{1,2}(t) V_{1,2}^*(t') \right] \Theta(t'-t)\end{aligned}\tag{A14}$$

where the mode functions must satisfy the homogeneous equations:

$$\frac{d^2 V_{1k}}{dt^2} + k^2 V_{1k}(t) - k \frac{e^2}{4\pi^2} \frac{\dot{\zeta}(t)}{f_\pi} V_{1k} = 0\tag{A15}$$

$$\frac{d^2 V_{2k}}{dt^2} + k^2 V_{2k}(t) + k \frac{e^2}{4\pi^2} \frac{\dot{\zeta}(t)}{f_\pi} V_{2k} = 0.\tag{A16}$$

The boundary conditions on the Green's functions, which include conditions of continuity and the KMS periodicity condition at finite initial temperature, allow all the constants – namely, the A's and the B's to be uniquely determined, finally yielding

$$\mathcal{G}_{jk}(t, t') = \mathcal{G}_{jk}^>(t, t') \Theta(t-t') + \mathcal{G}_{jk}^<(t, t') \Theta(t'-t)\tag{A17}$$

with the Wightman functions

$$\mathcal{G}_{jk}^>(t, t') = i \langle A_{Tj}^-(\vec{k}, t) A_{Tk}^+(-\vec{k}, t') \rangle\tag{A18}$$

$$= \left[\frac{P_{jk}}{2} \frac{1}{2ik} \{ (1+n_k) V_{1k}(t) V_{1k}^*(t') + n_k V_{1k}^*(t) V_{1k}(t') \} \right]$$

$$\begin{aligned}
& +(1 + n_k)V_{2k}(t)V_{2k}^*(t') + n_kV_{2k}^*(t)V_{2k}(t')\} \\
& -\frac{f_{jk}}{2}\frac{1}{2k}\{(1 + n_k)V_{1k}(t)V_{1k}^*(t') + n_kV_{1k}^*(t)V_{1k}(t') \\
& -(1 + n_k)V_{2k}(t)V_{2k}^*(t') - n_kV_{2k}^*(t)V_{2k}(t')\}]
\end{aligned}$$

and

$$\mathcal{G}_{jk}^{\leq}(t, t') = i\langle A_{Tj}^+(\vec{k}, t)A_{Tk}^-(-\vec{k}, t') \rangle \quad (\text{A19})$$

$$\begin{aligned}
& = \left[\frac{P_{jk}}{2}\frac{1}{2ik}\{(1 + n_k)V_{1k}^*(t)V_{1k}(t') + n_kV_{1k}(t)V_{1k}^*(t') \right. \\
& \quad \left. +(1 + n_k)V_{2k}^*(t)V_{2k}(t') + n_kV_{2k}(t)V_{2k}^*(t')\} \right. \\
& \quad \left. -\frac{f_{jk}}{2}\frac{1}{2k}\{(1 + n_k)V_{1k}^*(t)V_{1k}(t') + n_kV_{1k}(t)V_{1k}^*(t') \right. \\
& \quad \left. -(1 + n_k)V_{2k}^*(t)V_{2k}(t') - n_kV_{2k}(t)V_{2k}^*(t')\} \right].
\end{aligned}$$

Here, \vec{A}_T^+ and \vec{A}_T^- represent the transverse components of the gauge field along the forward and backward time contours of the closed time path integral.

REFERENCES

- [1] A. Anselm, Phys. Letters B217, 169 (1989); A. Anselm and M. Ryskin, Phys. Letters B226, 482 (1991); J. P. Blaizot and A. Krzywicki, Phys. Rev. D46, 246 (1992); Acta Phys. Polon. 27, 1687-1702 (1996) and references therein; J. D. Bjorken, Int. Jour. of Mod. Phys. A7, 4189 (1992); Acta Physica Polonica B23, 561 (1992). See also J. D. Bjorken's contribution to the proceedings of the ECT workshop on Disoriented Chiral Condensates, available at <http://www.cern.ch/WA98/DCC>; K. L. Kowalski and C. C. Taylor, "Disoriented Chiral Condensate: A white paper for the Full Acceptance Detector, CWRUTH-92-6; J. D. Bjorken, K. L. Kowalski and C. C. Taylor: "Observing Disoriented Chiral Condensates", (SLAC-CASE WESTERN preprint 1993) hep-ph/9309235 ; "Baked Alaska", (SLAC-PUB-6109) (1993); For recent reviews on the subject, see: K. Rajagopal, in *Quark Gluon Plasma 2*, ed. R. Hwa, World Scientific (1995); S. Gavin, Nucl. Phys. A590 (1995), 163c; J. P. Blaizot and A. Krzywicki, hep-ph/9606263 (1996); K. Rajagopal, hep-ph/9703258.
- [2] J. D. Bjorken, Phys. Rev. D27, 140, (1983); L. P. Csernai, "Introduction to Relativistic Heavy Ion Collisions", (John Wiley and Sons, England, 1994); C. Y. Wong, "Introduction to High-Energy Heavy Ion Collisions", (World Scientific, Singapore, 1994). H. Meyer-Ortmanns, Rev. of Mod. Phys. 68, 473 (1996).
- [3] K. Rajagopal and F. Wilczek, Nucl. Phys. B379, 395 (1993); K. Rajagopal and F. Wilczek, Nucl. Phys. B404, 577 (1993); S. Gavin, A. Goksch and R. D. Pisarski, Phys. Rev. Lett., 72, 2143 (1994); S. Gavin and B. Muller, Phys. Lett. B329, 486 (1994); Z. Huang and X. N. Wang, Phys. Rev. D49, 4335 (1994); P. F. Bedaque and A. Das, Mod. Phys. Lett A8, 3151 (1993); A. Abada and M. C. Birse, hep-ph/9612231.
- [4] J. Randrup, Phys. Rev. Lett. 77, (1996), LBL report 38125 (1995); 39328 (1996); hep-

- ph/9611228 (1996); hep-ph/9612453;
- [5] F. Cooper, Y. Kluger, E. Mottola and J. P. Paz, Phys. Rev. D51, 2377 (1995); Y. Kluger, F. Cooper, E. Mottola, J. P. Paz and A. Kovner, Nucl. Phys. A590, 581c (1995); M. A. Lampert, J. F. Dawson and F. Cooper, Phys. Rev. D54, 2213-2221 (1996), F. Cooper, Y. Kluger and E. Mottola, Phys. Rev. C 54, 3298 (1996); M. A. Lampert, J. F. Dawson and F. Cooper, Phys. Rev. D54, 2213 (1996).
- [6] D. Boyanovsky, H.J. de Vega and R. Holman, Phys. Rev. D51, 734 (1995).
- [7] D. Boyanovsky, H.J. de Vega, R. Holman and S. Prem Kumar, “Photoproduction Enhancement from Non-equilibrium Disoriented Chiral Condensates”, hep-ph/9701360.
- [8] D. Boyanovsky, M. D’Attanasio, H. J. de Vega and R. Holman Phys. Rev. D54, 1748 (1996).
- [9] H. Minakata, B. Muller, Phys. Lett. B 377:135-139, 1996.
- [10] S. Mrowczynski and B. Muller, Phys. Lett. B363, 1 (1995).
- [11] For pedagogical reviews on the Sigma model as an effective low energy theory, and its regime of validity see: V. Koch, *Aspects of Chiral Symmetry*, LBNL-39463-UC-413 (1996) and *Introduction to Chiral Symmetry* nucl-th/9512029 (Published in the Proceedings of TAPS Workshop, Bosen, Germany, Sep 1995. (unpublished).
- [12] *Dynamics of the Standard Model*, J. F. Donoghue, E. Golowich and B. R. Holstein, Cambridge University Press, Cambridge (1994).
- [13] R. D. Pisarski, in *From Thermal Field Theory to Neural Networks: a day to remember Tanguy Altherr*, Ed. P. Aurenche, P.Sorba and G. Veneziano (World Scientific, Singapore, 1996); Phys. Rev. Lett. 76, 3084 (1996); R. Baier, M. Dirks and O. Kober, Phys. Rev. D54, 2222 (1996); R. Pisarski and M. Tytgat, hep-ph/9702362 (1997).

- [14] F. Cooper and E. Mottola, *Mod. Phys. Lett. A* 2, 635 (1987); F. Cooper, S. Habib, Y. Kluger, E. Mottola, J. P. Paz, P. R. Anderson, *Phys. Rev. D* 50, 2848 (1994); F. Cooper, S.-Y. Pi and P. N. Stancioff, *Phys. Rev. D* 34, 3831 (1986); F. Cooper, Y. Kluger and E. Mottola hep-ph/9604284.
- [15] D. Boyanovsky, H. J. de Vega, R. Holman and S. Prem Kumar, in preparation.
- [16] F. Cooper, J. M. Eisenberg, Y. Kluger, E. Mottola, B. Svetitsky, *Phys. Rev. Lett.* 67, 2427 (1991); F. Cooper in “Particle Production in Highly Excited Matter”, Proceedings of the NATO ASI. ed. by H. Gutbrod and J. Rafelski (Plenum, New York 1993). F. Cooper, J. M. Eisenberg, Y. Kluger, E. Mottola, B. Svetitsky, *Phys. Rev. D* 48, 190 (1993); See also J. M. Eisenberg and Y. Kluger contributions in “Hot and Dense Nuclear Matter” Ed. by W. Greiner, H. Stocker and A. Gallmann (Nato Asi Series Plenum Press 1994) (pages 333 and 635).
- [17] D. Boyanovsky, H. J. de Vega and R. Holman, *Phys. Rev. D* 49, 2769 (1994); D. Boyanovsky, H. J. de Vega, R. Holman, D. S. Lee and A. Singh, *Phys. Rev. D* 51, 4419 (1995); D. Boyanovsky, H. J. de Vega, R. Holman, J. F. J. Salgado, *Phys. Rev.* 54, 7570 (1996).
- [18] J. Schwinger, *J. Math. Phys.* 2, 407 (1961); L. V. Keldysh, *JETP* 20, 1018 (1965); K. T. Mahanthappa, *Phys. Rev.* 126, 329 (1962); P. M. Bakshi and K. T. Mahanthappa, *J. Math Phys.* 41, 12 (1963).
- [19] K. Chou, Z. Su, B. Hao and L. Yu, *Phys. Rep.* 118, 1 (1985); A. Niemi and G. Semenoff, *Ann. of Phys. (NY)* 152, 105 (1984); N. P. Landsmann and C. G. van Weert, *Phys. Rep.* 145, 141 (1987); E. Calzetta and B. L. Hu, *Phys. Rev. D* 41, 495 (1990); *ibid* 37, 2838 (1990); J. P. Paz, *Phys. Rev. D* 41, 1054 (1990); *ibid* D 42, 529 (1990).
- [20] See for example: *A Course in Modern Analysis* by E. T. Whittaker and G. N. Watson,

Cambridge Univ. Press. 1920.

FIGURES

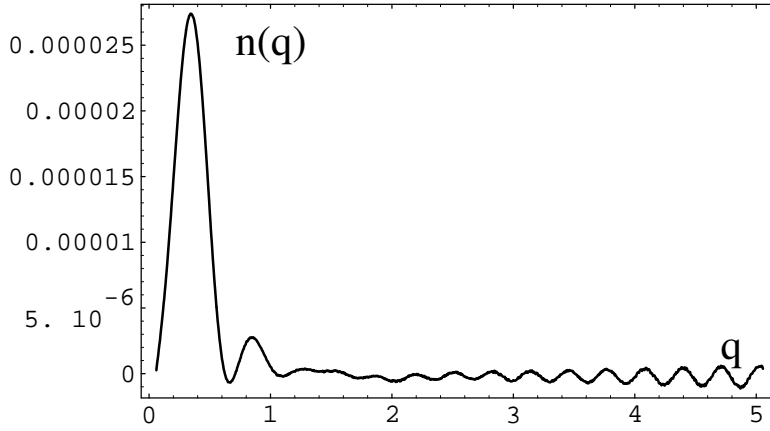


FIG. 1. $n(q, \tau) = (2\pi)^3 |q| \frac{d(N(\tau) - N(0))/\Omega}{d^3q}$ (in units of fm^{-1}), vs. q , at time $t = 10 \text{ fm}/c$, after subtracting the thermal background at $T_i = 220 \text{ MeV}$, for $\xi(0) = 0.1$, $\dot{\xi}(0) = 0$, $\phi(0) = \dot{\phi}(0) = 0$, $T_i = 220 \text{ MeV}$.

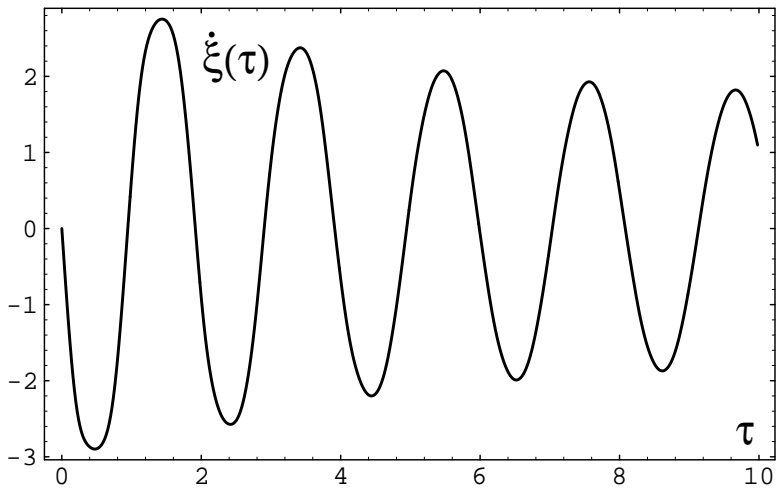


FIG. 2. (a) $\dot{\xi}(\tau)$ vs. τ (in units of fm/c) for $\xi(0) = 1.0$, $\dot{\xi}(0) = 0$, $\phi(0) = \dot{\phi}(0) = 0$, $T_i = 220$ MeV.

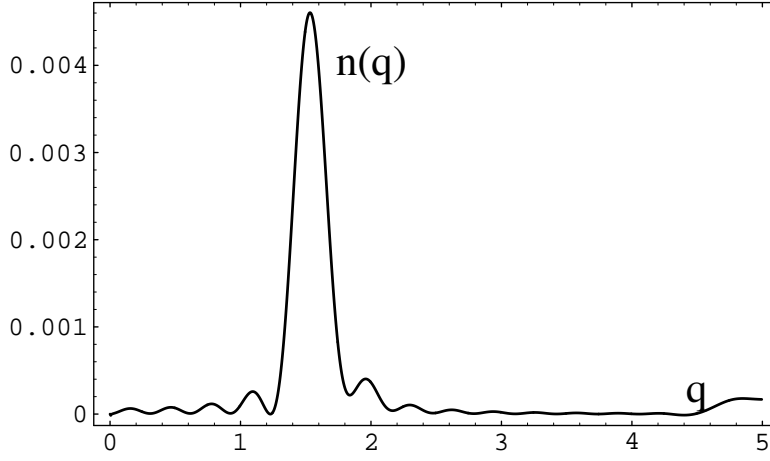


FIG. 2. (b) $n(q, \tau) = (2\pi)^3 |q| \frac{d(N(\tau) - N(0))/\Omega}{d^3q}$ (in units of fm^{-1}), vs. q , at time $t = 10 \text{ fm}/c$ for the same initial conditions as in Fig.(2.a).

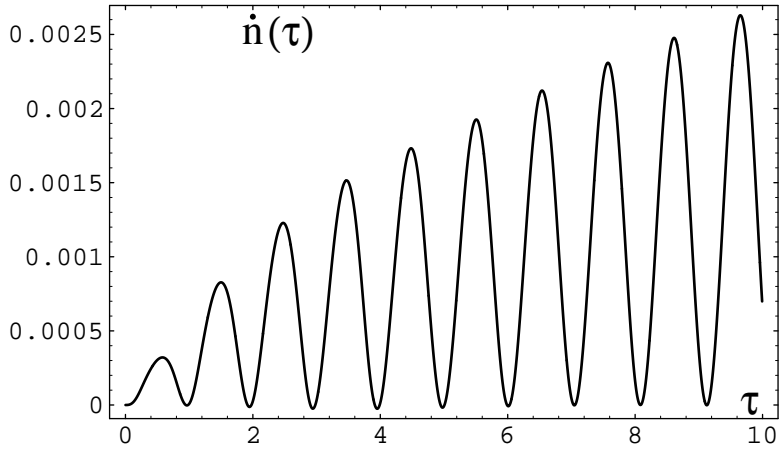


FIG. 2. (c) $\dot{n}(q, \tau) = (2\pi)^3 |q| \frac{d\dot{N}(\tau)/\Omega}{d^3q}$ (in units of fm^{-2}), at the center of the resonant band $qM_F = k = k_{res} = 306$ MeV as a function of τ (in units of fm/c), for the same initial conditions as in Fig.(2.a).

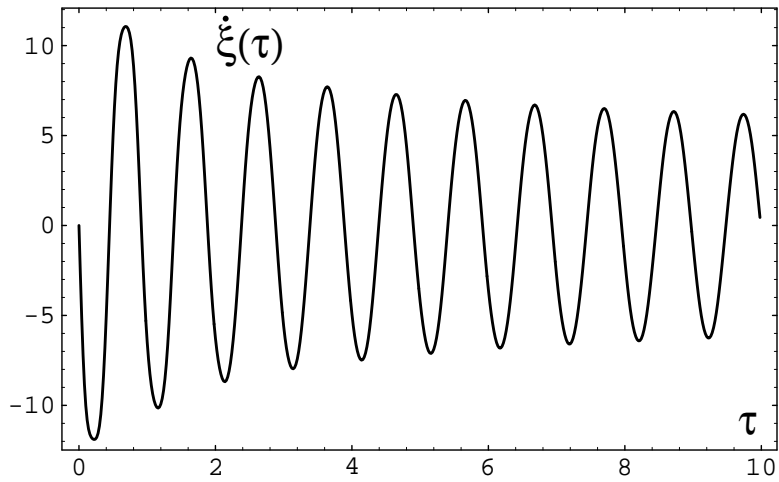


FIG. 3. (a) $\dot{\xi}(\tau)$ vs. τ (in units of fm/c) for $\xi(0) = 2.0$, $\dot{\xi}(0) = 0$, $\phi(0) = \dot{\phi}(0) = 0$, $T_i = 220$ MeV.

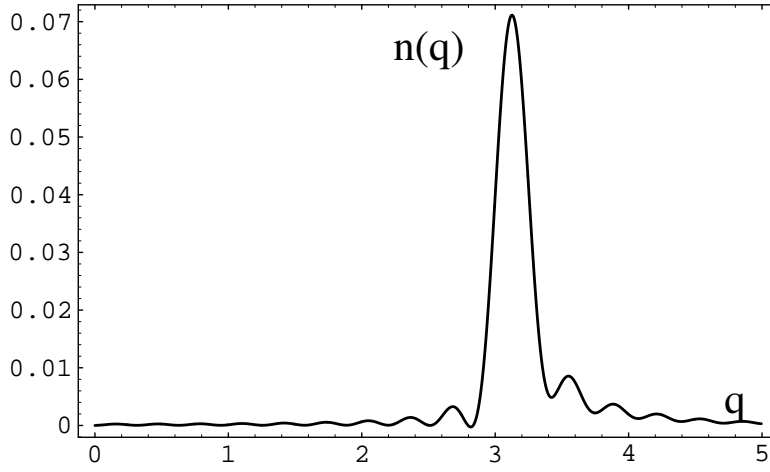


FIG. 3. (b) $n(q, \tau) = (2\pi)^3 |q| \frac{d(N(\tau) - N(0))/\Omega}{d^3q}$ (in units of fm^{-1}), vs. q , at time $t = 10 \text{ fm}/c$ for the same initial conditions as in Fig.(3.a).

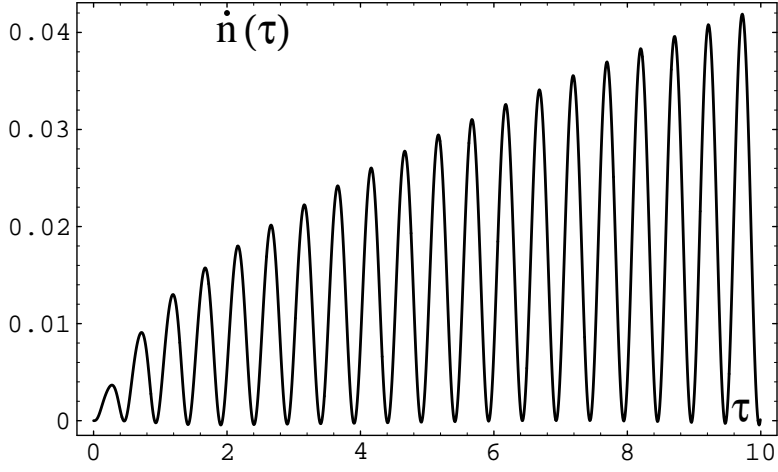


FIG. 3. (c) $\dot{n}(q, \tau) = (2\pi)^3 |q| \frac{d\dot{N}(\tau)/\Omega}{d^3q}$ (in units of fm^{-2}), at the center of the resonant band $qM_F = k = k_{res} = 625$ MeV as a function of τ (in units of fm/c), for the same initial conditions as in Fig.(3.a).

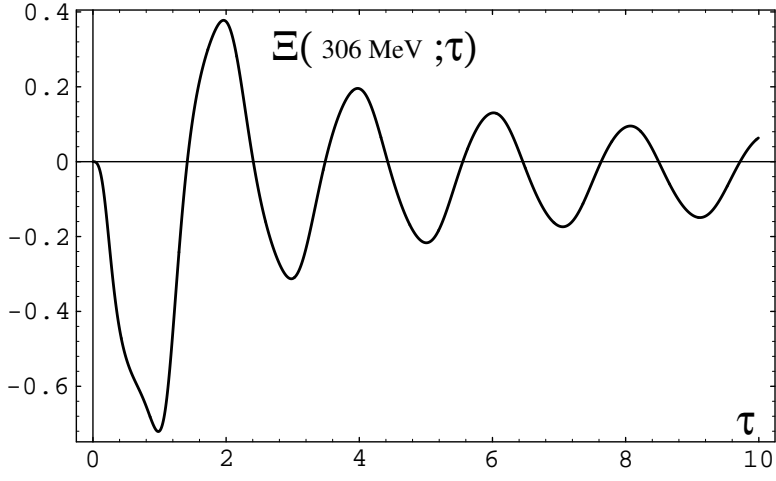


FIG. 4. (a) $\Xi(k = k_{res}, \tau) = (n_+ - n_-)/(n_+ + n_-)$ vs. τ (in units of fm/c), for $k = 306$ MeV and for the same initial conditions as in Fig.(2.a).

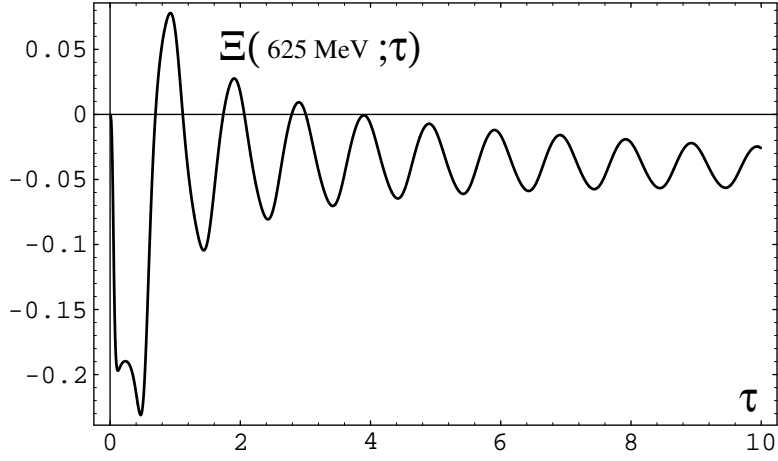


FIG. 4. (b) $\Xi(k = k_{res}, \tau) = (n_+ - n_-)/(n_+ + n_-)$ vs. τ (in units of fm/c), for $k = 625$ MeV and for the same initial conditions as in Fig.(3.a).

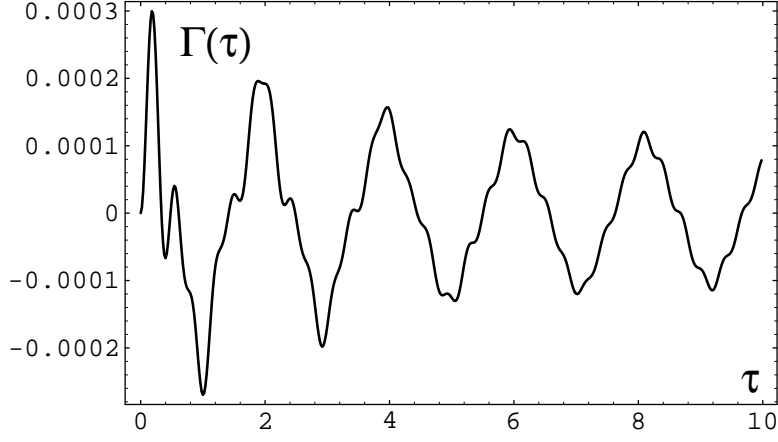


FIG. 5. (a) $\Gamma(\tau) = \alpha M_F \langle F \tilde{F} \rangle / 8\pi f_\pi$ (in units of M_F^4), vs. τ (in units of fm/c) for the initial conditions of Fig.(2.a).

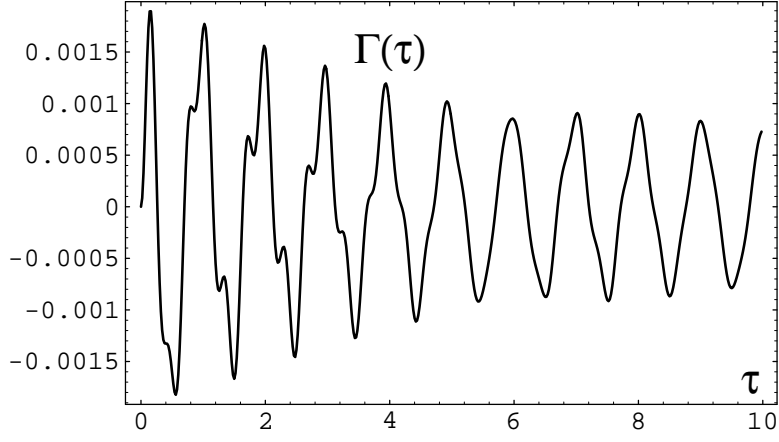


FIG. 5. (b) $\Gamma(\tau) = \alpha M_F \langle F \tilde{F} \rangle / 8\pi f_\pi$ (in units of M_F^4), vs. τ (in units of fm/c) for the initial conditions of Fig.(3.a).

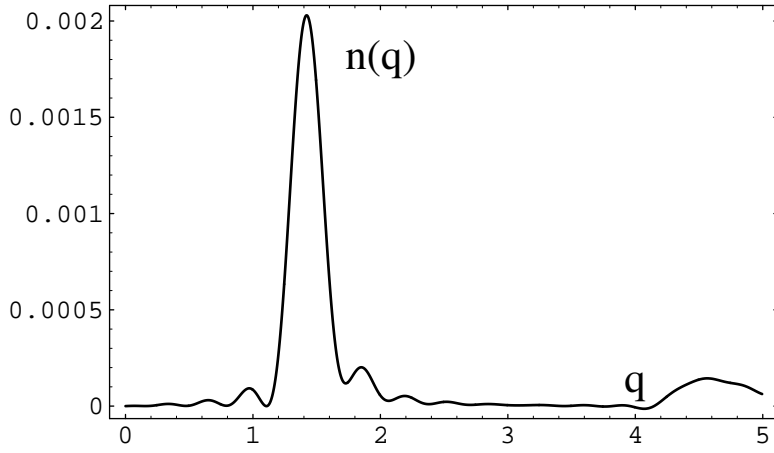


FIG. 6. (a) $n(q, \tau) = (2\pi)^3 |q| \frac{d(N(t) - N(0))/\Omega}{d^3 q}$ (in units of fm^{-1}), vs. q at time $t = 10 \text{ fm}/c$ for $\xi(0) = 1.0$, $\dot{\xi}(0) = 0$, $\phi(0) = \dot{\phi}(0) = 0$, $T_i = 0$.

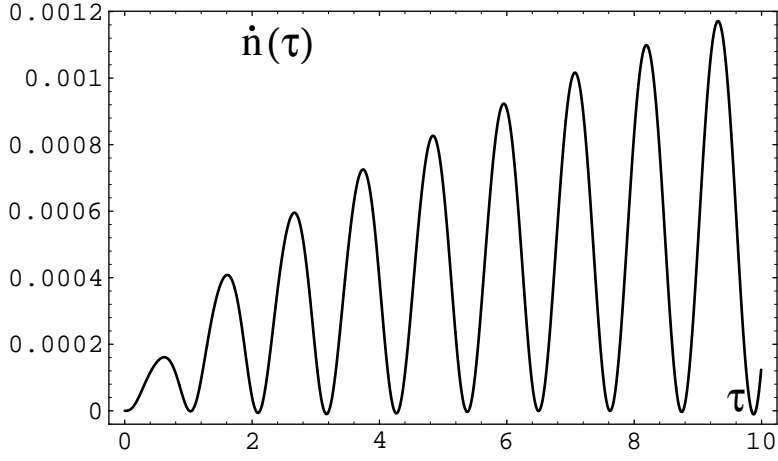


FIG. 6. (b) $\dot{n}(q, \tau) = (2\pi)^3 |q| \frac{d\dot{N}(t)/\Omega}{d^3q}$ (in units of fm^{-2}), at the center of the resonant band $qM_F = k = k_{res} = 284$ MeV as a function of τ (in units of fm/c) for the same initial conditions as in Fig.(6.a).

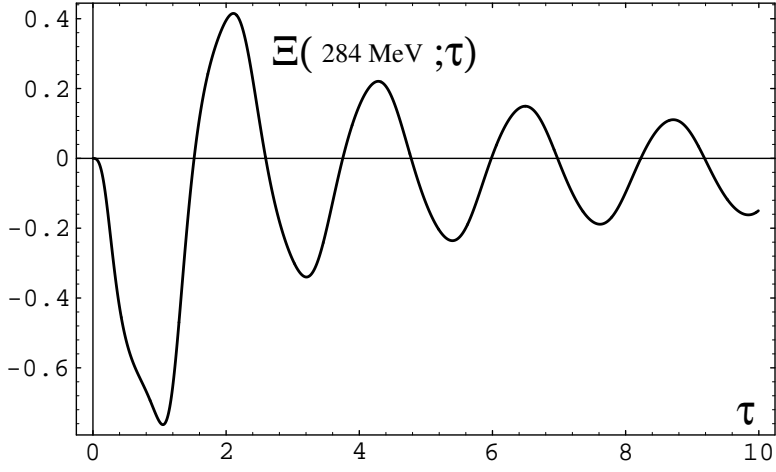


FIG. 6. (c) $\Xi(k = k_{res}, \tau) = (n_+ - n_-)/(n_+ + n_-)$ vs. τ (in units of fm/c), for $k = 284$ MeV and for the same initial conditions as in Fig.(6.a).